Evolution from a Molecular Rydberg Gas to an Ultracold Plasma in a Seeded Supersonic Expansion of NO

J. P. Morrison, C. J. Rennick, J. S. Keller,[*] and E. R. Grant[†]

Department of Chemistry, University of British Columbia, Vancouver, BC V6T 1Z3, Canada
(Received 14 April 2008; published 14 November 2008)

We report the spontaneous formation of a plasma from a gas of cold Rydberg molecules. Double-resonant laser excitation promotes nitric oxide, cooled to 1 K in a seeded supersonic molecular beam, to single Rydberg states extending as deep as 80 cm^{-1} below the lowest ionization threshold. The density of excited molecules in the illuminated volume approaches 1×10^{13} cm^{-3}. This population evolves to produce free electrons and a durable cold plasma of electrons and intact NO$^+$ ions.

Plasmas are usually hot, and thermal kinetic energy dominates in a binary-collision, gaslike fluid dynamics. However, under extreme conditions, many-body charged-particle interactions can exceed thermal energies and give rise to liquidlike or solidlike spatial correlations. The degree of correlation (Γ) depends on the translational energy of the ions compared with their Coulomb repulsion, which varies with plasma density as, $\Gamma = q^2/4\pi\varepsilon_0 akT$, where q is the charge, and a, the Wigner-Seitz radius, is related to the particle density, ρ, by, $4/3\pi a^3 = 1/\rho$ [1]. Strongly correlated plasmas ($\Gamma > 1$) are thought to exist at the center of heavy stars and under the conditions necessary for inertial confinement fusion.

Recent techniques for cooling distributions of atoms to ultracold temperatures have made it possible to approach the conditions of strong coupling in highly rarified systems in the laboratory [2]. Ultracold plasmas integrate atomic and mesoscopic domains, and thereby open the many-body multiscale heart of the problem to fundamental experimental and theoretical study [3–8].

Normal plasmas contain molecules as well as atoms, and molecular degrees of freedom affect their properties. Similarly, important questions can be raised concerning the role of molecular characteristics, such as rotational relaxation and cation-electron dissociative recombination, in directing the dynamics by which a gas of Rydberg molecules might evolve to form an ultracold plasma. However, a molecular ultracold plasma has yet to be produced for study.

Advances in research on atomic Rydberg gases and ultracold plasmas owe a great deal to the development of technology for producing cold atoms and atomic condensates in a magneto-optical trap (MOT) [9–12]. Rotational cycling prevents the laser deceleration of molecules, but one can routinely form dense molecular samples, cooled to temperatures of 1 K and less in seeded supersonic expansions.

While the molecules entrained in a supersonic beam are much warmer than the micro-Kelvin initial conditions typical in an atom trap, the plasma created in a MOT undergoes substantial excursions in temperature caused by disorder-induced heating followed by electron evaporation and Coulomb expansion [13,14].

By comparison, at a realistic excited-state density of 10^{12} cm^{-3}, electrons with a temperature as high as $T_e = 100$ K in the plasma formed by a Rydberg gas in the moving frame of a 1 K supersonic expansion would exhibit a correlation parameter approaching $\Gamma_e = 0.3$. The cation correlation in such a plasma could exceed 5 [9]. The evaporation of a carrier gas (typically He) presents a cooling mechanism not available in a MOT, improving the prospects for higher correlation.

The realization of a cold molecular plasma under such conditions would represent a significant development. A great many small molecules can be seeded in free jets, and this medium would thus represent an important new platform for the broader study of Rydberg gas to ultracold plasma dynamics. Rydberg gases of alkali atoms have been known for some time to form plasmas under the warmer conditions of an effusive beam [15]. But, for molecular systems, there remains the important question of predissociation and dissociative recombination: Can a molecular ultracold plasma form, and if so, how long can it survive?

In results reported here, we establish that excited NO molecules in ensembles of photoselected Rydberg states lying more than 80 cm^{-1} below the lowest ionization threshold can interact in a supersonic molecular beam to produce a cold plasma that is long lived and remarkably durable.

In our experiment, a pulsed jet of NO, which is seeded at 10% in He at a backing pressure of 5 atm, expands through a 0.5 mm diameter nozzle. Two centimeters downstream, an electroformed Ni skimmer selects the 1 mm diameter core of this free jet to form a differentially pumped supersonic molecular beam.

This stagnation pressure and nozzle diameter predict a seeded jet in which the He carrier has a terminal speed ratio of about 90, which gives rise to a parallel temperature of approximately 700 mK for its NO component [16], where we can understand this $T_\parallel^\infty$ to be the second moment of the

longitudinal velocity distribution function under the terminal conditions of free molecular flow.

Translational cooling of the NO is accompanied by rotational cooling as well, but, because rotational relaxation occurs with a smaller collision cross section, its equilibration ceases before the onset of molecular flow, with the result that the terminal rotational temperature, T_R^∞, exceeds $T_\parallel^\infty$.

The centerline intensity for an ideal isentropic expansion relates proportionally to the nozzle flow rate by

$$I_0 = \frac{\kappa}{\pi} F(\gamma) n_0 \sqrt{\frac{2kT_0}{m}} \left(\frac{\pi d^2}{4} \right),$$

where κ and $F(\gamma)$ are the peaking factor and heat capacity function, which for our conditions have values of 1.98 and 0.51, respectively [17]. n_0 and T_0 are the stagnation density and temperature, and d is the nozzle diameter. For a pure He beam under present conditions, this approximation predicts $I_0 = 9 \times 10^{21}$ particles s^{-1} sr^{-1}. Allowing for attenuation by the skimmer, this flux yields an instantaneous density of 4.8×10^{14} particles cm^{-3} at a distance 10.5 cm from the nozzle.

Addressing a small volume element at this distance, our experiment excites entrained NO molecules by the sequential application of unfocused 5 ns pulses, ω_1 and ω_2, from two frequency-doubled Nd:YAG-pumped dye lasers. First-photon absorption in the region of 226 nm promotes transitions in the $A^2\Sigma^+ - X^2\Pi \gamma$ (0,0) system.

At laser pulse energies greater than 500 μJ, a scan of ω_1 yields the resonant two-photon ionization spectrum of this band system, detected in the electron signal. Line intensities reflect the population of ground-state rotational levels, determined by T_R^∞. For the conditions described above we typically observe a rotational temperature in the range of 3 K.

Tuning to the specific transition from $X^2\Pi v'' = 0$, $N'' = 1 (J'' = \frac{1}{2})$ to $A^2\Sigma^+ v' = 0$, $N' = 0 (J' = \frac{1}{2})$, we decrease the power of ω_1 until the electron signal from one-color resonant two-photon ionization disappears. At this point, the $A^2\Sigma^+ - X^2\Pi$ first step is still saturated, and we overlap a second laser pulse, ω_2, to further excite these photoselected NO molecules. Scanning ω_2 over the range from 30 400 to 30 530 cm^{-1} populates high-Rydberg states in series converging to the lowest ionization threshold of NO.

To estimate the absolute density of excited-state molecules produced under our conditions, we scale the total density at the interaction distance by the seeding ratio (0.1), the rotational fraction in $J'' = \frac{1}{2}(-)$ at 3 K (0.44), and two factors of 0.5 for saturated steps of ω_1 and ω_2 excitation. From this, we obtain an approximate density of high-Rydberg NO molecules of 5×10^{12} cm^{-3}.

Excited molecules formed in this illuminated volume move with the jet through a nominally field-free region to reach an exit grid, G_2, as diagrammed in Fig. 1. At certain frequencies of ω_2 well below the two-color ionization threshold of NO, the combination of laser pulses at ω_1 and ω_2 produces an electron signal waveform exemplified by Fig. 2. This waveform consists of a prompt electron signal, which appears at the MCP within about 200 ns of ω_2 excitation, followed by a broader pulse of electrons that arrives 8.2 μs later.

The shape and arrival time of the prompt pulse depends slightly on the magnitude of the very low dc field applied between grids 1 and 2. At zero field, the prompt peak reaches the detector 250 ns after ω_2. When we bias G_1 to form a weak 250 mV acceleration field, the prompt electron signal sharpens to arrive at 170 ns, as in Fig. 2, while the delayed signal remains unaffected. If we bias the flight tube and detector to form a cation time-of-flight mass spectrometer, we find the same delayed-peak waveform with a flight-time offset corresponding to the mass of NO$^+$.

The amplitude of the delayed electron pulse depends on the magnitude of the dc voltage applied to the flight-tube entrance grid, G_3, rising from zero with no gradient between G_2 and G_3, to plateau slightly higher than relative intensity shown for gradients above 100 V/cm.

For a given G_3 voltage, the intensity of this late signal does not vary to a large degree with Rydberg binding energy, and, most significantly, yields comparable numbers of electrons for $\omega_1 + \omega_2$ energies below and above the G_3 field-ionization limit. From this result, we can conclude that, by the time the illuminated volume reaches G_2, it has
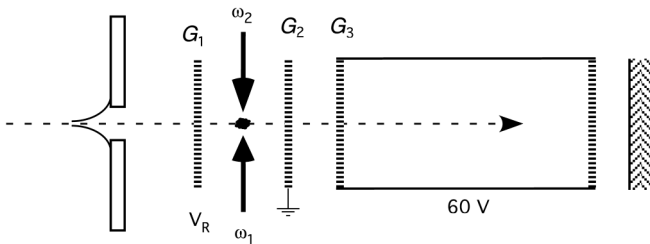

FIG. 1. Schematic diagram showing the molecular beam flight path from a differentially pumped source chamber through a skimmer to enter a system of three grids ending in a flight tube capped by a microchannel plate detector. Approximately to scale with the G_1 to G_2 spacing of 2 cm.
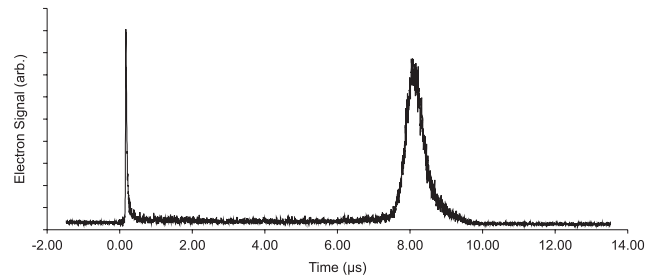

FIG. 2. Oscilloscope trace showing the arrival time of electrons produced following two-color production of NO molecules in the $52f(2)$ Rydberg state with -250 mV applied to G_1 and 60 V applied to G_3.

lost memory of the principal quantum number, n, to which it was initially excited. We take this to indicate that the Rydberg molecules prepared by $\omega_1 + \omega_2$ excitation have evolved to form a plasma, and that this plasma has survived for the 8.2 μs required to reach G_2.

The intensity profile of this signal reflects electrons extracted from this plasma volume as it passes through G_2, which produces a waveform reflecting the velocity of the molecular beam in the laboratory frame. Thus, for a measured distance of 11 mm from the the laser interaction region to G_2 the peak arrival time in Fig. 2 corresponds to average velocity of 1340 m/s. This figure conforms well with the value of $\bar{V}_{\parallel}^{\infty} = 1358$ m/s predicted for a 90:10 mixture of He and NO.

The breadth of this waveform is determined by the width of our illumination volume, which is about 1 mm or 10% of the flight distance to G_2.

The integrated electron signal collected as a function of ω_2 forms a spectrum of the Rydberg series populated by second-photon absorption. We can readily assign this spectrum to the nf Rydberg series of NO converging to the $v^+ = 0$, $N^+ = 2$ state of $^1\Sigma$ NO^+. In the region of $\omega_2 = 30\,490$ cm^{-1}, a few lines appear in the np series converging to the $N^+ = 0$ rotational level of the cation ground state.

The Rydberg states of NO predissociate with rates of decay that vary by series according to orbital angular momentum, l, and along a series with principal quantum number, n. For n from 40 to 70, isolated-molecule lifetimes in the nf series converging to $N^+ = 2$ range from 10 to 30 ns. Intrinsic lifetimes for np states fall below 1 ns for $n < 70$. The inhomogeneous electrostatic fields presented by neighboring ions cause l and m_l mixing, which can lengthen these lifetimes appreciably.

Previous investigators have characterized these properties of the high-Rydberg states of NO by means of double-resonant laser excitation followed by pulsed-field ionization [18]. In our experiment, resonant absorption is signaled by the prompt production of free electrons, in the absence of a pulsed field, at total energies as much as 80 cm^{-1} (10 meV) below the lowest ionization threshold of NO. This behavior closely parallels the emission of electrons from atomic Rydberg gases comparably prepared in optical traps [9–14].

When we apply an electrostatic pulse in our apparatus (e.g., for $n = 50$, a pulse of 1 μs duration and amplitude 30 V/cm, delayed 500 ns), we produce an instantaneous field-ionization response, but the delayed signal we associate with plasma electrons remains.

We can reverse the polarity of the field-ionization pulse with similarly no effect on the plasma signal. In fact, we can apply delayed, reverse-bias pulses as high as 150 V/cm, and observe surprisingly little effect on the signal produced by electrons released when the illuminated volume passes G_2, even though the amplitude of such a pulse substantially exceeds the field-ionization

threshold for all the principal quantum numbers in this range.

Figure 3 shows a sequence of spectra obtained by collecting the plasma signal present following the application of reversed polarity field-ionization pulses with amplitudes ranging from 5 to 125 V/cm. This experimental result again supports the notion that our Rydberg gas has evolved to form a cold plasma. Note, in particular, that the electron signal extracted by the passage of the active volume into a field of 60 V cm^{-1} appears undiminished even after the application of a pulsed field at more than twice this gradient. The plasma resists destruction by an electrostatic potential that is well in excess of the field-ionization threshold of the underlying Rydberg states, and then regeneratively sheds electrons in response to the subsequent smaller field gradient encountered at G_2.

We can understand this property of the plasma in terms of its predicted Debye screening length. Assuming that Rydberg-Rydberg, Penning interactions promote electrons in one-half of the NO Rydberg states in our sample, and fewer than 1% of these electrons escape the active volume, an electron density, n_e, of 2×10^{12} cm^{-3} would remain. Allowing for electron temperatures as high as $T_e = 100$ K, we obtain a Debye screening length, $\lambda_D = \sqrt{\epsilon_0 k T_e / q_e^2 n_e} < 0.5$ μm, far smaller than the width of our active volume, a point of scale marking the onset of collective effects. Thus, the second field gradient at G_2 extracts electrons that have redistributed from the core of the plasma to its surface in the time following the reverse-bias pulse at 1 μs.

While the plasma signal is remarkably robust to the application of a several hundred V/cm field-ionization pulse a half-microsecond or more after ω_2, an electrostatic pulse of much lower amplitude, applied in coincidence with ω_2 (at $t = 0$) completely extinguishes the late signal. When this pulse is applied with increasing delay after $t = 0$, the late signal grows, reaching its field-free ampli-
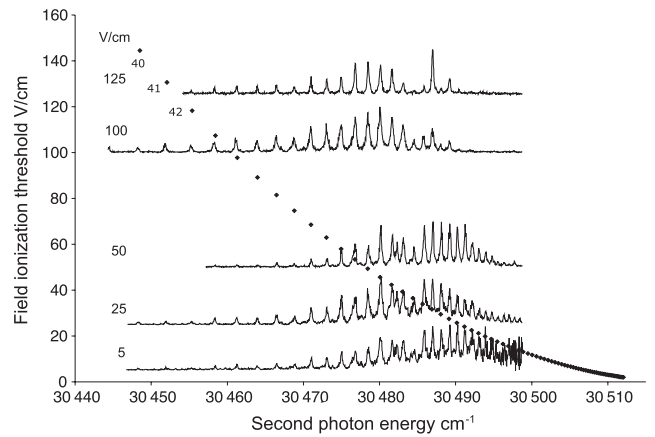

FIG. 3. High-Rydberg excitation spectra of the plasma signal under conditions in which 1 μs positive pulses at voltages producing the electrostatic fields indicated are applied starting 500 ns after ω_2. Diamonds show the adiabatic field-ionization threshold for the principal quantum numbers from 40 to 110.

tude after 200 ns. The rise time of the signal as a function of pulse delay follows a second-order rate law, in accordance with a Rydberg-Rydberg collisional energy-pooling mechanism.

We find that both the amplitude and this pulsed-field-measured appearance time for a durable plasma signal depends on the properties of the initially prepared population of high-Rydberg NO molecules. If the density of excited molecules, which can be regulated by the delay between ω_1 and ω_2, is too low, we see no plasma signal. If the temperature of NO in the molecular beam, as reflected by its rotational line intensities in the ω_1 spectrum, is too high, we see no plasma signal. If the principal quantum number selected by double resonance is too low, we see no plasma signal.

Energy conservation demands energy pooling for the production of free electrons and a plasma from an ensemble of NO molecules that have initial energies below the ionization threshold. Density and n-dependent orbital radius clearly regulate the encounter frequency by which this can occur.

Temperature in the molecular beam may have a twofold effect. Increased rotational temperature reduces the density of excited molecules, because it spreads the rotational distribution into states that are not promoted by double-resonant excitation. In addition, it is possible that attractive intermolecular interactions drive disproportionating Rydberg-Rydberg electronic energy transfer in NO, analogous to the dipole-dipole coupling that ignites ultracold plasmas in cold gases of Rydberg atoms [19]. In this case, a higher $T_{\parallel}^{\infty}$ could be expected to inhibit plasma formation.

Finally, we return to the question of dissociative recombination. The energy per excited NO molecule in our sample greatly exceeds the thermochemical threshold to form N ^{4}S and O ^{3}P. Dissociation to neutral atoms represents a dissipation path at all stages of this experiment. Results presented above suggest that the Rydberg gas in our system evolves to a plasma on a timescale of 200 ns. Intrinsic predissociation lifetimes are found to be much shorter than this. Lifetime lengthening by l and m_l mixing in the inhomogeneous fields of nearby ions must operate under our conditions to close this relaxation channel.

A similar dynamics must apply for dissociative recombination, the rate of which is well established for NO under binary-collision conditions. This rate increases with decreasing cation-electron collision energy. For an electron temperature of 100 K, theory and experiment predict the lifetime of a single NO$^+$ cation to be 700 ns at the electron density of our plasma [20]. At such a rate, bimolecular cation-electron recombination would extinguish the plasma long before it reached G_2. The plasma environment, with its inhomogeneous field of incompletely shielded charges, must operate to admix high-l partial waves in cation-electron scattering states, resulting in an-

gular momentum barriers that block core penetration to inhibit dissociative recombination, much like predissociation is inhibited for discrete states. The plasma environment has been seen directly to mix l and m_l in atomic systems, with consequences for delayed electron photoemission [7,10]. A similar many-body electrodynamics likely accounts for the durability of our ultracold molecular plasma.

---

*Permanent address: Department of Chemistry, Kenyon College, Gambier, OH 43022-9623, USA.
†Author to whom correspondence should be addressed.
edgrant@chem.ubc.ca

[1] S. Ichimaru, Rev. Mod. Phys. **54**, 1017 (1982).
[2] T. Killian, T. Pattard, T. Pohl, and J. Rost, Phys. Rep. **449**, 77 (2007).
[3] T. Amthor, M. Reetz-Lamour, C. Giese, and M. Weidemüller, Phys. Rev. A **76**, 054702 (2007).
[4] F. Robicheaux, J. V. Hernández, T. Topçu, and L. D. Noordam, Phys. Rev. A **70**, 042703 (2004).
[5] M. S. Murillo, Phys. Plasmas **14**, 055702 (2007).
[6] C. Ates, T. Pohl, T. Pattard, and J. M. Rost, Phys. Rev. A **76**, 013413 (2007).
[7] B. Knuffman and G. Raithel, Phys. Rev. A **75**, 053401 (2007).
[8] P. J. Tanner, J. Han, E. S. Shuman, and T. F. Gallagher, Phys. Rev. Lett. **100**, 043002 (2008).
[9] T. C. Killian, S. Kulin, S. D. Bergeson, L. A. Orozco, C. Orzel, and S. L. Rolston, Phys. Rev. Lett. **83**, 4776 (1999).
[10] D. Feldbaum, N. V. Morrow, S. K. Dutta, and G. Raithel, Phys. Rev. Lett. **89**, 173004 (2002).
[11] A. Walz-Flannigan, J. R. Guest, J.-H. Choi, and G. Raithel, Phys. Rev. A **69**, 063405 (2004).
[12] W. Li, M. W. Noel, M. P. Robinson, P. J. Tanner, T. F. Gallagher, D. Comparat, B. LaburtheTolra, N. Vanhaecke, and T. Vogt *et al.*, Phys. Rev. A **70**, 042713 (2004).
[13] J. L. Roberts, C. D. Fertig, M. J. Lim, and S. L. Rolston, Phys. Rev. Lett. **92**, 253003 (2004).
[14] R. S. Fletcher, X. L. Zhang, and S. L. Rolston, Phys. Rev. Lett. **99**, 145001 (2007).
[15] G. Vitrant, J. Raimond, M. Gross, and S. Haroche, J. Phys. B **15**, L49 (1982).
[16] D. R. Miller, in *Atomic and Molecular Beam Methods*, edited by G. Scoles (Oxford University Press, New York, 1988), p. 14.
[17] H. C. W. Beijerinck and N. F. Verster, Physica (Amsterdam) **111B+C**, 327 (1981).
[18] M. Vrakking and Y. Lee, J. Chem. Phys. **102**, 8818 (1995).
[19] W. Li, P. J. Tanner, and T. F. Gallagher, Phys. Rev. Lett. **94**, 173001 (2005).
[20] I. F. Schneider, I. Rabadán, L. Carata, L. H. Andersen, A. Suzor-Weiner, and J. Tennyson, J. Phys. B **33**, 4849 (2000).